

Solubilization and anticancer-activity enhancement of Methotrexate by novel dendrimeric nanodevices synthesized in one-step reaction

Delia Soto-Castro^a, Jorge A. Cruz-Morales^a, María Teresa Ramírez Apan^b, Patricia Guadarrama^{a,*}

^a Instituto de Investigaciones en Materiales, Universidad Nacional Autónoma de México, Apartado Postal 70-360, CU, Coyoacán, México DF 04510, Mexico

^b Instituto de Química, Universidad Nacional Autónoma de México, Apartado Postal 70-213, CU, Coyoacán, México DF 04510, Mexico

ARTICLE INFO

Article history:

Received 17 November 2011

Available online 27 January 2012

Keywords:

Dendrimers
Nanodevices
Methotrexate
Conjugates
Encapsulation

ABSTRACT

The one-step synthesis of nanodevices based on PAMAM framework for targeted cancer therapy is described. Four water-soluble nanodevices (named fractions **F1** to **F4**) were rightly separated by size discrimination, and characterized. From biological assays of cell growth inhibition percentage, the anticancer activity of Methotrexate (chemotherapeutic drug) as part of a nanodevice, generally increases over cancer cell lines and notably, in case of human lymphocytes, the cell growth inhibition percentage decreases drastically (more than 80%), thus, the nanodevices exhibited a favorable discrimination between healthy and diseased cells. From the characterization it can be conclude that the synthesized nanodevices provide a dual scenario of drug transportation: encapsulation and conjugation.

© 2012 Elsevier Inc. All rights reserved.

1. Introduction

Several polymers have been extensively studied as drug delivery vehicles, especially for anticancer drugs [1,2]. The use of nanodevices, within the so called macromolecular therapy (MT), allows a number of therapeutic, pharmacokinetic and pharmaceutical advantages in comparison to conventional low-molecular weight therapeutics with free drugs [3-8].

Among the macromolecules likely to be used in MT, monodisperse dendrimers are prime candidates, with a great versatility due to their unique architecture and functionality at nanoscale [9,10]. There are generally two different scenarios of transport/delivery of drugs where dendrimers have been tested; the encapsulation by non-covalent interactions [11,12] and the formation of conjugates [13] (drug molecules covalently attached to a macromolecule). Both scenarios lead to increased solubility of the drugs and a lessened cytotoxicity; however, in case of encapsulation, the control of the delivery rate is difficult to accomplish [14]. This can be a disadvantage when prolonged periods of delivery-time are required, but it can turn into an advantage since high concentrations of drug can be provided in short periods of time [15]. In case of conjugates [4,5,7], the drug accumulation becomes more selective and the circulation time in the body is larger, but it must be taken into account that there is a limit of hydrophobic drug loading, in order to avoid the formation of a molecular entity too hydrophobic to be soluble in physiologic media.

The well-known PAMAM (polyamidoamine) dendrimers have been modified as conjugates with Methotrexate (anti-metabolite

drug used in chemotherapy) and folic acid (targeting agent) covalently linked, allowing therapeutic responses, not possible to get with the free drug [16,17]. In order to reduce the cytotoxicity from terminal amines, and prevent non-specific reactions at the periphery of PAMAM, pegylation or acetylation reactions were carried out [18]. The possible modification of the PAMAM surface, keeping the nanoscale dimensions, high water solubility and biocompatibility, place these macromolecules as excellent candidates in drug-carrying processes.

In this paper is described the one-step synthesis of nanodevices based on PAMAM framework for targeted cancer therapy, including Methotrexate (MTX) as chemotherapeutic drug, and folic acid (FA) as target agent. FA was chosen to preferentially target cancer cells that have folate receptors expressed on their surfaces, and improve the transit across the cell membranes. After the modification of the PAMAM periphery with tris(hydroxymethyl) aminomethane (TRIS), low stoichiometric ratios of MTX and FA were loaded in order to maintain a proper hydrophobic/hydrophilic balance. From the characterization it can be conclude that novel nanodevices with dual behavior of drug transportation (encapsulation and conjugation) in the same entity were obtained. The quantification of MTX and FA molecules was determined by NMR and UV-vis spectroscopy. In vitro assays of the new nanodevices on different cancer cell lines show anticancer-activity enhancement of Methotrexate.

2. Materials and methods

2.1. Chemistry

Chemicals were obtained from commercial sources and used without further purification. DMSO were dried over CaH₂ (5% w/

* Corresponding author.

E-mail address: patriciagua@iim.unam.mx (P. Guadarrama).

v) overnight, filter and freshly distilled at reduced pressure prior to use. NMR spectra were recorded on a Bruker Avance 400. FT-IR spectra were measured on a Nicolet 6700 spectrometer. MS (FAB) mass spectra were measured Jeol JSM AX102A spectrometer. UV-vis spectra were recorded using a UNICAM UV 300 UV/vis Spectrometer Vision 32 software, in phosphates buffer solution (PBS) at pH 7.4.

2.2. Tetramethyl 3,3',3'',3'''-(ethane-1,2-diylbis(azanetriyl))tetrapropanoate (1)

2 g (33 mmol) of ethylenediamine (ETDA) are diluted in 30 mL of methanol. The flask is sealed, purged and isolated from light. Then 14.3 mL (158 mmol) of methyl acrylate are injected and the reaction was allowed to elapse for 48 h. The reaction was monitored by thin layer chromatography using ethyl acetate as eluent, until the mark for ethylenediamine disappears. The reaction mixture is concentrated under vacuum to obtain the product as translucent oil in quantitative yield.

FT-IR (cm^{-1}): 2946, 2821 (C–H aliph.) 1733 (C=O). NMR ^1H ($\delta(\text{ppm})$): (Acetone- d_6 , 2.05): 2.43 (t, 8H, $-\text{CCH}_2\text{COO}-$, $J = 6.98$ Hz); 2.51 (s, 4H, $-\text{N}(\text{CH}_2)_2\text{N}-$), 2.75 (t, 8H, $-\text{NCH}_2\text{C}-$, $J = 6.98$ Hz), 3.61 (s, 12H, $-\text{COOCH}_3$). ^{13}C ($\delta(\text{ppm})$): (Acetone- d_6 , 30.56); 34.28 ($-\text{CCH}_2\text{COO}-$), 51.67 ($-\text{NCH}_2\text{C}-$), 52.54 ($-\text{COOCH}_3$), 54.11 ($-\text{N}(\text{CH}_2)_2\text{N}-$), 174.2 ($-\text{CCOOC}-$). FAB + m/z calc. 405.5; m/z exp.405.5.

2.3. PAMAM-G1 (2)

2 g (4.9 mmol) of compound 1 dissolved in 20 mL of methanol and added dropwise to a solution of 22.3 g (371 mmol) of ethylenediamine (ETDA) in 50 mL of methanol (the flask is purged and isolated from light). The reaction proceeds by 7 days at room temperature. The reaction mixture was concentrated and repeatedly washed with *t*-BuOH to remove ETDA until it is undetected by GC.

2.4. PAMAM-G1.5 (3)

2.3 g (4.45 mmol) of tetra-amine product 2 was dissolved in 30 mL of methanol, the flask is purged, isolated from light and 3.9 mL (42.7 mmol) of methyl acrylate are injected. The reaction was left for 48 h, after which the reaction mixture was concentrated to obtain the dendrimer 3 as amber oil. Two steps yield: 95%.

FT-IR (cm^{-1}): 3304 (NH); 2951, 2823 (C–H aliph.); 1729, 1644 (C=O); NMR (Acetone- d_6) ^1H ($\delta(\text{ppm})$): 2.46 (t, 24H, $-\text{CCH}_2\text{COO}-$, $-\text{CCH}_2\text{CON}-$, $J = 6.83$ Hz); 2.56 (t, 8H, $-\text{CCH}_2\text{N}-$, $J = 6.53$ Hz), 2.76 (t, 20H, $-\text{NCH}_2\text{C}-$, $-\text{N}(\text{CH}_2)_2\text{N}-$, $J = 6.83$ Hz), 2.88 (t, 8H, $-\text{NCH}_2\text{C}-$, $J = 6.83$ Hz), 3.24 (t, 8H, $-\text{CONHCH}_2\text{C}-$, $J = 6.43$ Hz), 3.64 (s, 24H, $-\text{COOCH}_3$). ^{13}C ($\delta(\text{ppm})$): (Acetone- d_6); 33 ($-\text{CCH}_2\text{CON}-$, $-\text{CCH}_2\text{COO}-$), 38 ($-\text{CONHCH}_2\text{C}-$), 49 ($-\text{NCH}_2\text{C}-$, $-\text{COOCH}_3$), 52 ($-\text{NCH}_2\text{C}-$), 53 ($-\text{CCH}_2\text{N}-$), 54 ($-\text{N}(\text{CH}_2)_2\text{N}-$), 172 ($-\text{CCONH}-$), 173 ($-\text{CCOOC}-$). ESI (+MS) m/z calc. (1206.4); m/z exp. 1206.0.

2.5. PAMAM-G2.5 (4)

0.5 g (2.9 mmol) of dendrimer 3 ($G = 1.5$) were dissolved in 40 mL of methanol and added slowly to a solution of 48 g (798.6 mmol) of ETDA. After 9 days at room temperature, the mixture is concentrated and washed repeatedly with *t*-BuOH to remove the remaining ETDA. Then 3.3 g (2.3 mmol) of eight-amine product was dissolved in 60 ml of methanol, the flask is purged, isolated from light, and 4 ml (44.3 mmol) of methyl acrylate are injected. The reaction was left for 48 h, after which the mixture is

concentrated to obtain the dendrimer 4 as amber oil. Yield of two steps: 92%.

FT-IR (cm^{-1}): 3305.1 (NH); 2951.7, 2823.5 (C–H aliph.); 1729.9, 1643.1 (C=O). NMR (CDCl_3) ^1H ($\delta(\text{ppm})$): 2.36 (t, 24H, $-\text{CCH}_2\text{CON}-$, $J = 6.50$ Hz), 2.43 (t, 32H, $-\text{CCH}_2\text{COO}-$, $J = 6.60$ Hz), 2.50–2.61 (m, 28H, $-\text{CCH}_2\text{N}-$, $-\text{N}(\text{CH}_2)_2\text{N}-$), 2.74 y 2.80 (2t, 56H, $-\text{NCH}_2\text{C}-$, $J = 6.70$ Hz y $J = 6.61$ Hz), 3.22 a 3.30 (m ancho, 24H, $-\text{CONHCH}_2\text{C}-$), 3.62 (s, 48H, $-\text{COOCH}_3$). ^{13}C ($\delta(\text{ppm})$): (CDCl_3); 31.2 ($-\text{CCH}_2\text{CON}-$); 32.6 ($-\text{CCH}_2\text{COO}-$), 37.2 ($-\text{CONHCH}_2\text{C}-$), 49.2 ($-\text{NCH}_2\text{C}-$, $-\text{CCH}_2\text{N}-$); 49.7 ($-\text{CCH}_2\text{N}-$, $-\text{N}(\text{CH}_2)_2\text{N}-$); 51.7 (COOCH_3), 52.8 ($-\text{NCH}_2\text{C}-$), 171 ($-\text{CCONH}-$), 173 ($-\text{CCOOC}-$). ESI (+MS) calc. 2807.6; exp.2807.9.

2.6. PAMAM-TRIS (5)

A suspension of tris(hydroxymethyl) aminomethane (TRIS; 1.03 g; 8.54 mmol) is prepared in 15 mL of methanol, and a solution of 1 g (0.35 mmol) of dendrimer 4 in 5 mL of methanol is added, heating to boiling point for 7 days, until the FT-IR band around 1733 cm^{-1} , associated to methyl ester carbonyl disappears. The reaction mixture is concentrated to obtain amber oil that is dissolved in the minimum amount of water and precipitated with acetone. This procedure was repeated several times to get a slightly yellow solid product, extremely hygroscopic. Yield: 70%.

FT-IR (cm^{-1}): 3287.4(NH, OH), 2938.8 (C–H aliph.) 1635.1 (C=O). NMR (D_2O) ^1H ($\delta(\text{ppm})$): 2.36–2.42 (m, 56H, $-\text{CCH}_2\text{COO}-$); 2.54–2.70 (m, 36H, $-\text{CCH}_2\text{N}-$, $-\text{N}(\text{CH}_2)_2\text{N}-$), 2.74–2.87 (m, 56H, $-\text{NCH}_2\text{C}-$), 3.25–3.34 (m, 36H, $-\text{CONHCH}_2\text{C}-$); 3.74 (s, 96, $-\text{CCH}_2\text{OH}$). ^{13}C ($\delta(\text{ppm})$): (D_2O); 33.55 ($-\text{CCH}_2\text{COO}-$), 37.22 ($-\text{OCNHCH}_2\text{C}-$), 49.52 ($-\text{NCH}_2\text{C}-$), 50.46 ($-\text{N}(\text{CH}_2)_2\text{N}-$), 51.79 ($-\text{CCH}_2\text{N}-$), 61.33 ($-\text{C}(\text{CH}_2\text{OH})_3$), 62.42 ($-\text{HNC}(\text{CH}_2\text{OH})_3$), 175.75 ($-\text{CCONH}-$).

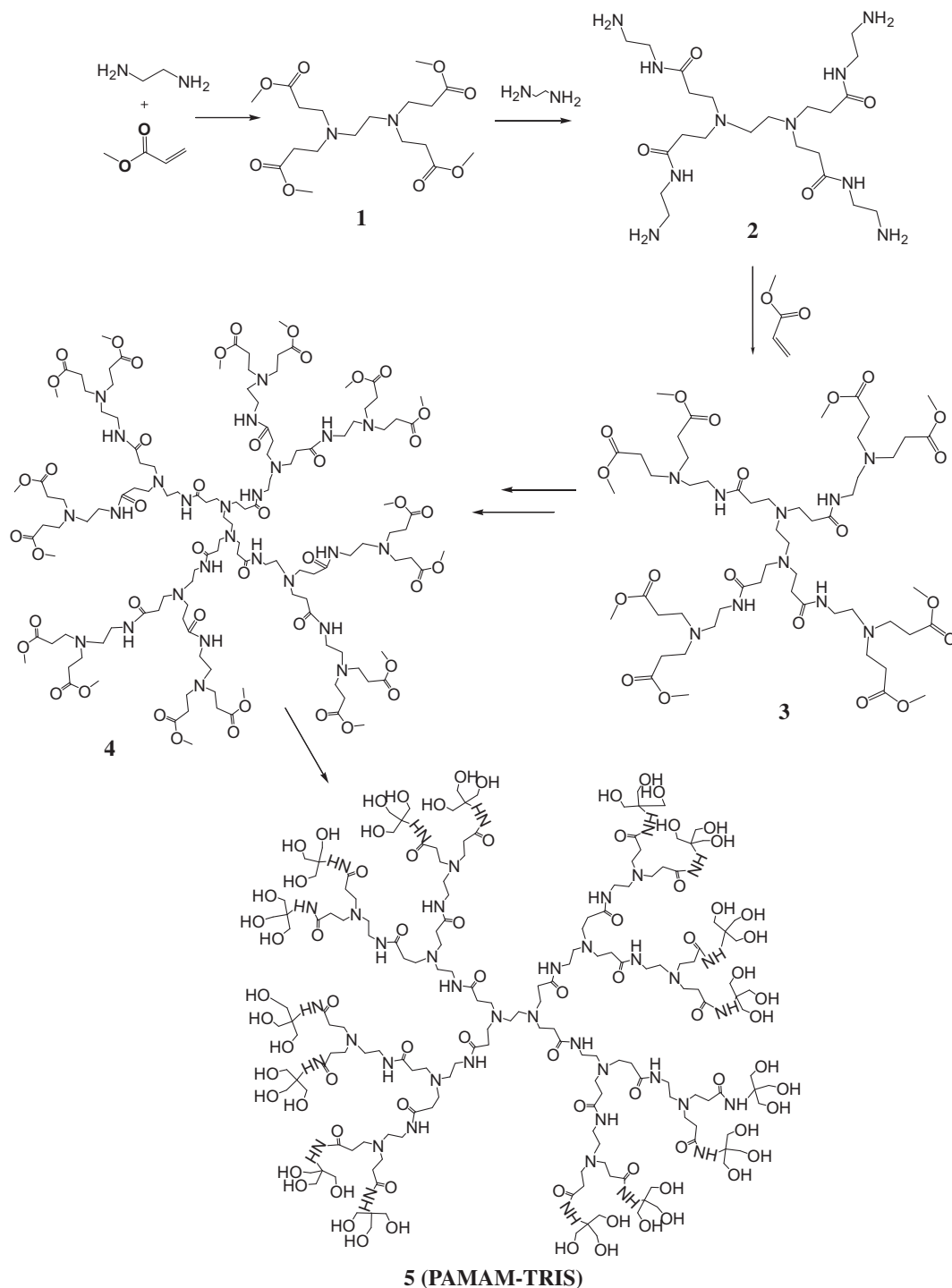
2.7. Nanodevices

In a flask previously purged with Ar, 0.5 g (0.1187 mmol) of PAMAM-TRIS and 17.7 mg (0.145 mmol) of 4-*N,N*-Dimethylamino-pyridine (DMAP, 0.33 eq. respect to esterified COOH groups) were dissolved in 15 mL of DMSO. Separately, in containers purged with Ar, 0.1 g (0.22 mmol) of MTX and 0.1 g (0.22 mmol) of FA are dissolved in 10 ml of DMSO each. A solution of DCC (108.9 mg, 0.528 mmol) was prepared separately in 3 mL of DMSO. The flask with PAMAM-TRIS and DMAP remains with vigorous stirring and slow (in a period of 3 h) and simultaneously are added MTX, AF and DCC in solution. After the addition the reaction is left for 48 h at room temperature, after which the mixture was concentrated under reduced pressure and re-dissolved in 3 mL of MeOH to precipitate unreacted DCU, FA and MTX, and remove by filtration. Viscous oil (0.82 g) is obtained and re-dissolved in 1 mL of methanol/3 drops of water, to be passed through a Sephadex-LH20 column, eluting with MeOH. The separation by size discrimination allows four water soluble fractions of low polydispersity and removes the remaining DCU, FA and MTX (see Scheme 1).

2.8. Biological assays

2.8.1. Cell lines culture and culture medium

The dendrimers were screened in vitro against human cancer cell lines: HCT-15 (human colorectal adenocarcinoma), MCF-7 (human mammary adenocarcinoma), K562 (human chronic myelogenous leukemia), U251 (human glioblastoma), PC-3 (human prostatic adenocarcinoma), SKLU-1 (human lung adenocarcinoma), cell lines were supplied by National Cancer Institute (USA). Besides human lymphocytes MT2 cell lines, the human tumor cytotoxicity was also determined by using the proteinbinding dye sulforhodamine B (SRB) in microculture assay to measure cell growth as described in



Scheme 1. Synthesis of PAMAM G2.5 and its functionalization with TRIS at the periphery.

the protocols established by the NCI [19]. The cell lines were cultured in RPMI-1640 medium supplemented with 10% fetal bovine serum, 2 mM L-glutamine, 10,000 units/ml penicillin G sodium, 10,000 µg/ml streptomycin sulfate and 25 µg/ml amphotericin B (Gibco) and 1% non-essential amino acids (Gibco). They were maintained at 37 °C in humidified atmosphere with 5% CO₂. The viability of the cells used in the experiments exceeded 95% as determined with trypan blue.

2.8.2. Cytotoxicity assay

Cytotoxicity after treatment of the tumors cells and normal cell with the test compounds was determined using the protein-binding

dye sulforhodamine B (SRB) in microculture assay to measure cell growth as described in the reference of Monks et al. 1991 [19]. The cells were removed from the tissue culture flasks by treatment with trypsin, and diluted with fresh media. From these cell suspension, 100 µL containing 5000–10,000 cell per well, were pipetted into 96 well microtiter plates (Costar) and the material was incubated at 37 °C for 24 h in a 5% CO₂ atmosphere. Subsequently, 100 µL of a solution of the dendrimers obtained by diluting the stocks were added to each well. The cultures were exposed for 48 h to the compound at concentrations 50 µM. After the incubation period, cells were fixed to the plastic substratum by the addition of 50 µL of cold 50 % aqueous trichloroacetic acid. The plates

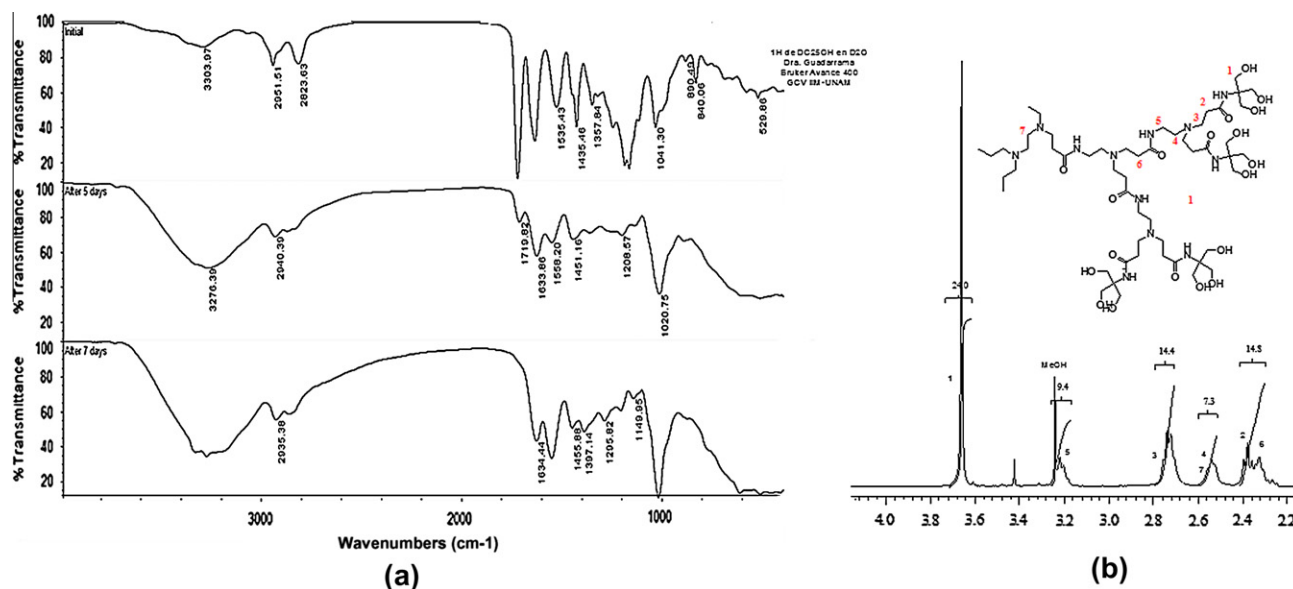


Fig. 1. (a) FT-IR spectra showing the evolution of the functionalization of PAMAM G2.5 with TRIS in MeOH; (b) NMR ^1H spectrum of PAMAM-TRIS.

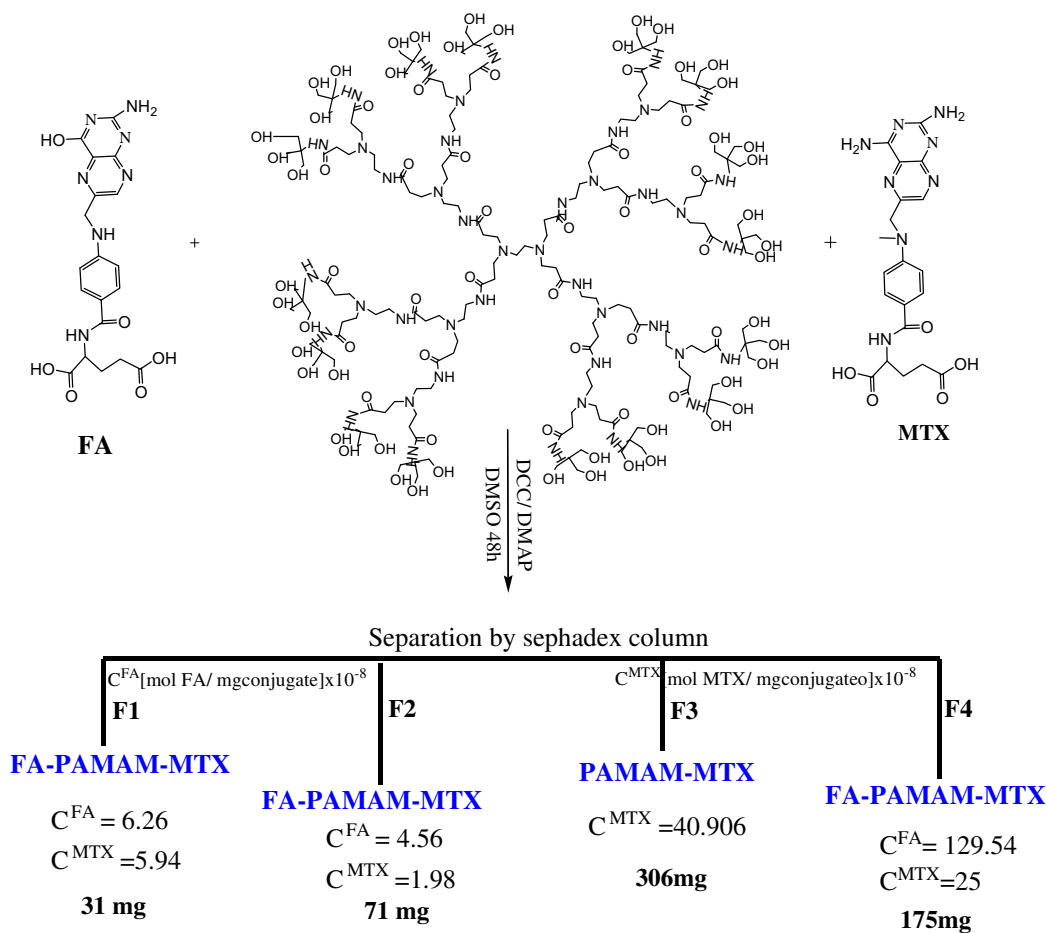


Fig. 2. Synthesis of nanodevices and proportional concentration of FA/MTX determined by UV-vis.

were incubated at 4 °C for 1 h, washed with tap H₂O, and air-dried. The trichloroacetic-acid-fixed cells were stained by the addition of 0.4% SRB. Free SRB solution was then removed by washing with 1% aqueous acetic-acid. The plates were then air-dried, and the

bound dye was solubilized by the addition of 10 mM unbuffered Tris base (100 μL). The plates were placed on a shaker for 5 min, and the absorption was determined at 515 nm using an ELISA plates reader (BioTex Instruments).

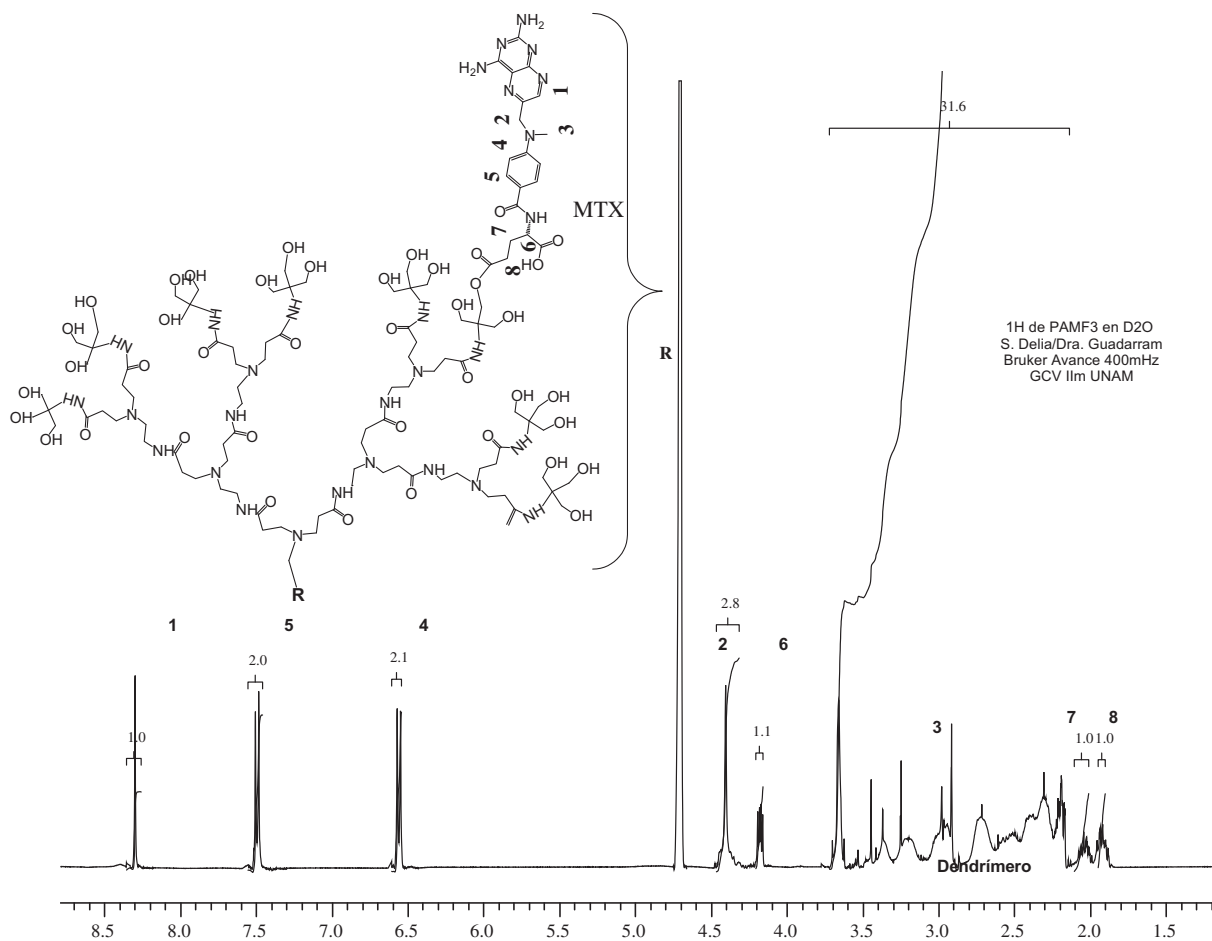


Fig. 4. NMR ^1H spectrum of **F3** in D_2O .

the formation of a major fraction containing only MTX. It is worth mentioning that, although the reaction was carried out in DMSO, pKa data can be extrapolated because, regardless of the dielectric constant of the solvent, the tendency remains.

Fractions **F1** and **F2** are viscous oils, while **F3** and **F4** are yellow solids. By their appearance is confirmed that fractions **F1** and **F2** have a very low load of MTX and FA, thus maintaining the physical properties of the dendrimer PAMAM-TRIS, while fractions **F3** and **F4**, with a much heavier load of MTX and FA, retain the physical properties of these molecules (yellow solids).

The four fractions obtained, clearly are vehicles to enhance the solubility of both MTX and FA, and can be considered as nanodevices for drug-carriage.

3.2. Characterization of nanodevices

FT-IR spectra of all fractions are similar. Characteristic bands in $2100\text{--}3500\text{ cm}^{-1}$ due to carboxylic acids from FA/MTX were observed. A band around 3270 cm^{-1} , corresponding to terminal hydroxyl groups from PAMAM-TRIS is also present. A broad band in 1565 cm^{-1} is assigned to carbonyls from amide groups (PAMAM-TRIS/FA/MTX conjugates). Illustratively, spectra of the PAMAM-TRIS, FA and fraction **F3** (with only MTX) are shown in Fig. 3.

The IR spectra of fractions **F1** and **F2** show two bands in 3324 cm^{-1} and 2926 cm^{-1} , presumably due to encapsulated DCU, therefore, these fractions were not considered for further biological assays.

From the ^1H NMR spectrum of fraction **F3** (Fig. 4), two well defined regions are observed: an aromatic region where three signals corresponding to MTX are located in 8.4 ppm (singlet, peridine ring), 6.65 ppm and 7.6 ppm, related to protons of the aromatic ring. The other region contains overlapping signals from dendrimer PAMAM-TRIS and drug molecule. As will be corroborated below by UV-vis, **F3** contains only MTX molecules linked to PAMAM-TRIS.

Regarding the second most abundant fraction; **F4**, according to NMR (^1H , Fig. 5) both molecules, FA and MTX are present and distinguished by the signals corresponding to the respective aromatic rings, a doublet in 6.64 ppm assigned to two of the protons of FA, and the doublet in 6.75 ppm assigned to the counterpart in MTX. The ratio between signals allows for a 5 to 1 stoichiometry of molecules of FA and MTX, respectively, which is confirmed by UV-vis.

Thus, by NMR was possible to discriminate fractions with different contents of FA and MTX, and these fractions exhibit very different behaviors in assays *in vitro*, as shown below.

As mentioned before, some of the fractions correspond to nanodevices with a dual behavior of carrier (encapsulation and conjugation) in the same entity. From the NMR spectra, signals around 3.9 ppm are assigned to the methylenes of TRIS already esterified, which accounts for molecules of MTX/FA covalently anchored, forming conjugates (as example, see NMR spectrum from **F1**; Supporting information). On the other hand, signals between 2.2 and 3.8 ppm, corresponding to PAMAM-TRIS, exhibit a splitting due to two different chemical environments assignable to “free” dendrimer, and dendrimer encapsulating FA/MTX molecules via non-covalent interactions (see spectra from Figs. 4 and 5). Accord-

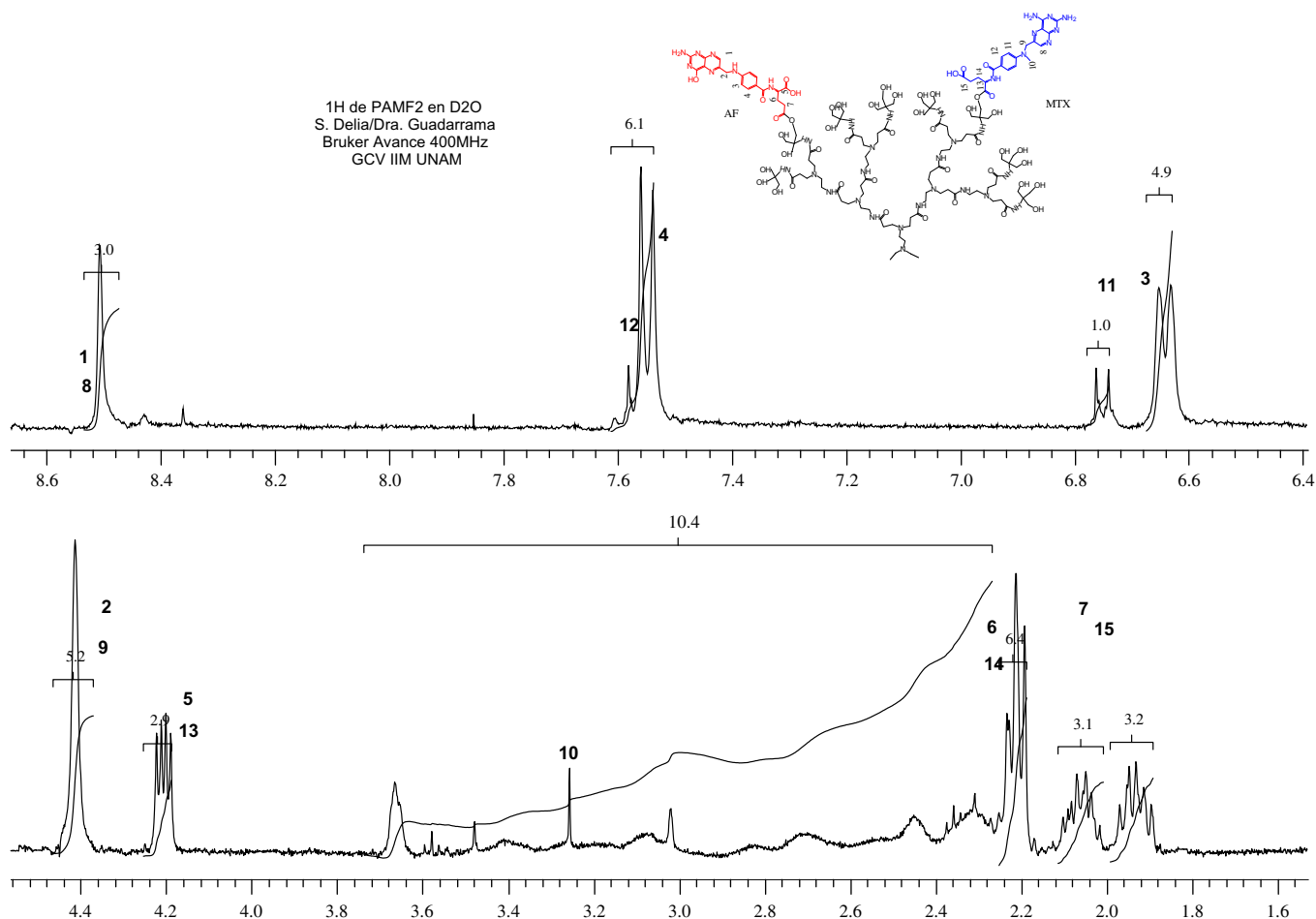


Fig. 5. NMR ^1H spectrum of **F4** in D_2O .

ing to integral ratio of the signals in 8.50 and 3.66 ppm (corresponding to the proton of pteridine ring of MTX/FA, and methylene protons of TRIS, respectively), the MTX:PAMAM-TRIS ratio is 42:1 for fraction **F3** and 103:1 for fraction **F4** (containing both, MTX and FA). Such a high charge of MTX/FA per dendrimer can only be explained by the formation of supramolecular structures mediated by non-covalent interactions, which are still completely soluble in aqueous media. Mass spectra for these fractions were attempted by ESI-MS, but the fragmentation patterns led to misleading conclusions. Future work includes mass determinations by MALDI-TOF.

From UV-vis spectra of nanodevices (measured in phosphates buffer solution (PBS) at pH 7.4; Fig. 6), with the exception of **F3**, all fractions contain both FA and MTX, anchored/encapsulated to PAMAM-TRIS.

To determine the average molar concentrations of MTX in fraction **F3**, the Lambert-Beer law together with the calibration curve of MTX, measured at 304 nm (Fig. 7), was used.

It is important to mention that the absorption maxima of FA and MTX overlap, thus is not possible to quantify directly the concentration of each analyte; therefore, in case of **F1**, **F2** and **F4** containing FA and MTX, it was considered the additive character of the Lambert-Beer's law for binary mixtures and the concentrations were determined as detailed in support information, the results are summarized in Table 1.

Thus, in case of fraction **F4** is corroborated the 5:1 ratio of FA:MTX by UV-vis, as was observed above by NMR.

It is important to mention that the nanodevices are stable in aqueous solutions, in dark and dryness conditions, at room temperature for several months. When the concentrations of FA and MTX are determined after these periods of time, they remain the same.

3.3. Biological section

3.3.1. Pamam tris

Since non-cytotoxicity is a necessary attribute for any biomaterial, the harmlessness of dendrimer PAMAM-TRIS was evaluated by assays on human lymphocytic cells (MT2) [23]. The results, obtained in triplicate by Monks protocol (see Ref. [19]), as well as the standard error, are shown in Table 2. A sample of polyglycidol was included as reference of innocuity [24].

Although the main interest for the biological study was the verification of non-cytotoxicity of the new materials in normal cell lines, additional assays on human cancer cell lines were carried out for forthcoming studies.

In Table 2, the + sign denotes cell growth compared with the control, which means that the compounds are non cytotoxic; and the values without + sign correspond to cell growth inhibition percentage.

From these results it can be observed that dendrimer PAMAM-TRIS, exhibits cytotoxicity towards two cancer cell lines only, and is harmless towards normal cells. Even though polyglycidol (refer-

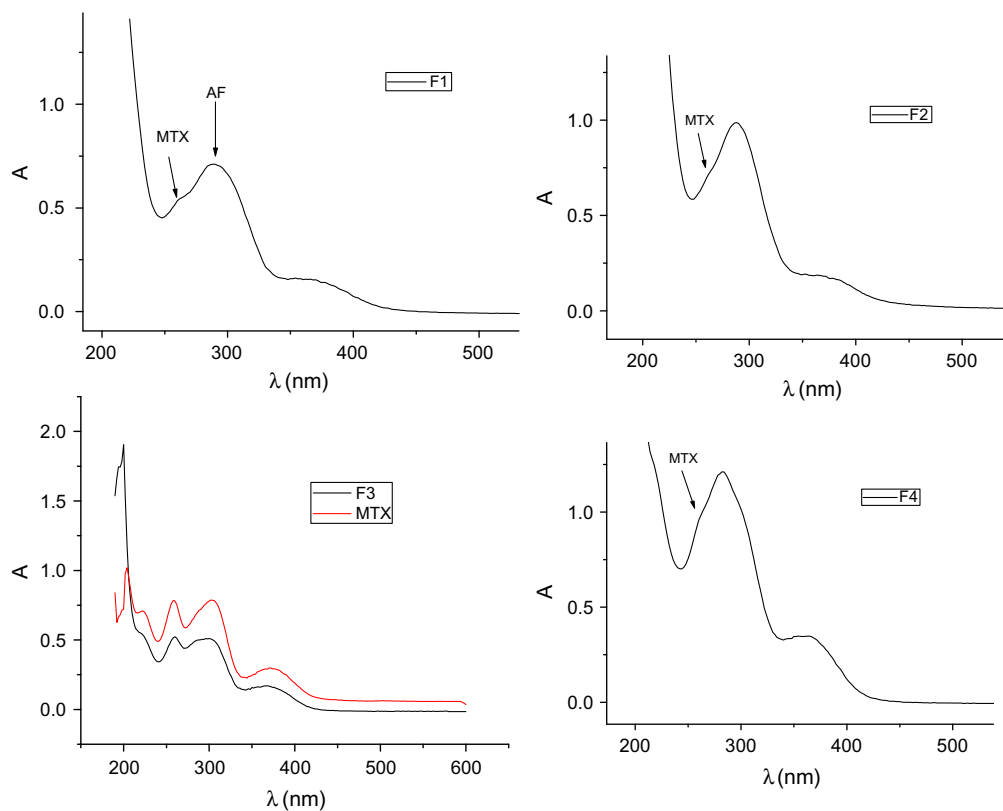


Fig. 6. UV-vis spectra of fractions **F1** to **F4** in phosphate buffer solution (pH 7.4). **F3** and MTX (red) spectra are shown together.

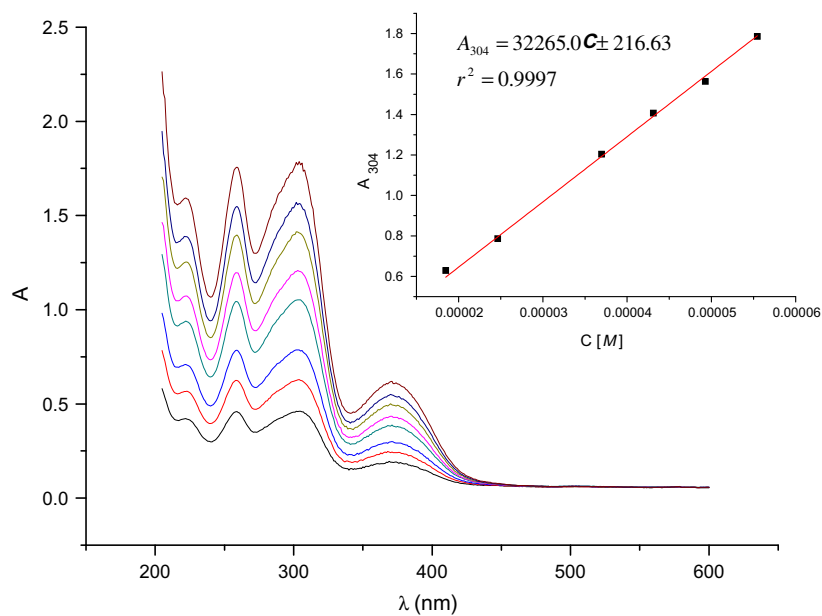


Fig. 7. Absorption spectra of MTX in PBS buffer at pH 7.4 and calibration curve at 304 y 370 nm in a concentration range of 1.8×10^{-5} to 5.5×10^{-5} M.

Table 1
Average concentrations of FA and MTX in fractions **F1** to **F4**.

	$C^{FA} \times 10^4$ M	$C^{MTX} \times 10^4$ M	$C^{FA} \times 10^8$ M/mg	$C^{MTX} \times 10^8$ M/mg
F1	0.3633	0.3444	6.264	5.938
F2	0.2919	0.1265	4.561	1.977
F3	–	1.15	–	40.91
F4	2.33	0.47	129.54	25.95

ence compound) showed cytotoxicity in some cancer cell lines, it was also non cytotoxic towards normal cells (lymphocytes).

3.3.2. Nanodevices

In order to evaluate the cytotoxic behavior of MTX embedded in dendrimeric nanodevices, assays were conducted to determine the cell growth inhibition percentage in different cancer cell lines and human lymphocytes cell line (MT2). The results of Table 3 shows that the MTX activity not only is maintained but increases, except

Table 2Cell growth inhibition percentage of human cancer cell lines and human lymphocytic cells^a.

Compound	MT2	U251	PC-3	K-563	HCT-15	MCF7	SKLU-1
PAMAM-TRIS	+8.7 ± 2.7	+14.7 ± 2.1	+3.89 ± 1.2	+17.1 ± 5.1	+6.7 ± 5.9	4.6 ± 3.7	12.7 ± 1.6
Polyglycidol ^b	+5.8 ± 0.6	1.6 ± 0.1	+5.4 ± 1.8	6.4 ± 0.08	4.8 ± 1.5	5.3 ± 0.2	5.5 ± 1.5

^a Cellular activity measured in presence of different compounds at 50 μM ± standard error. MT2: Human lymphocytes; Human cancer cell lines: U251 (human glioblastoma); PC-3 (human prostatic adenocarcinoma); K562 (human chronic myelogenous leukemia cells); HCT-15 (human colorectal adenocarcinoma); MCF-7 (human mammary adenocarcinoma); SKLU-1 (human lung adenocarcinoma).

^b MW = 4591; polydispersity = 1.8.

Table 3Cell growth inhibition percentage of human cancer cell lines and human lymphocytic cells^a.

Sample	MT-2	U251	PC-3	K562	HCT-15	MCF-7	SKLU-1
MTX	86.34	61.8 ± 3.3	27.9 ± 5.6	44.0 ± 4.1	55.1 ± 2.4	50.6 ± 2.9	54.1 ± 1.9
F3	16.47 ± 5.1	87.7 ± 6.0	18.4 ± 1.1	47.0 ± 4.2	94.4 ± 6.5	89.5 ± 10.6	67.2 ± 7.6
F4	+3.5 ± 3.8	88.8 ± 1.7	7.1 ± 0.1	41.7 ± 5.4	96.1 ± 1.8	87.9 ± 5.5	64.7 ± 3.8

^a Cell growth inhibition percentage measured in presence of different compounds at 50 μM ± standard error. MT2: Human lymphocytes; Human cancer cell lines: U251 (human glioblastoma); PC-3 (human prostatic adenocarcinoma); K562 (human chronic myelogenous leukemia cells); HCT-15 (human colorectal adenocarcinoma); MCF-7 (human mammary adenocarcinoma); SKLU-1 (human lung adenocarcinoma); ^bMW = 4591; polydispersity = 1.8.

for cell line of prostatic cancer; PC-3. It is noteworthy that, in case of human lymphocytes, the cell growth inhibition percentage decreases drastically (more than 80%) in presence of fraction **F3** containing only MTX, and fraction **F4** containing FA and MTX, promotes growth of this cell line, presumably due to the presence of FA, which acts as a metabolite. According to the results, the nanodevices, with or without FA, will discriminate between healthy and diseased cells.

4. Conclusions

Novel dendrimeric nanodevices for cancer therapy were synthesized in one step reaction, starting from PAMAM functionalized in the periphery with TRIS through a practical adaptation to existing protocol. The used methodology allows the obtaining of fractions easily separable by size discrimination that can be characterized by common spectroscopic techniques. The MTX concentration (in presence or absence FA) is exactly determined by UV–vis.

Considering purity and composition, nanodevices named as fractions **F3** and **F4** were of interest for biological testing. From cell growth inhibition percentage assays, the anticancer activity of MTX, as part of a nanodevice, generally increases over cancer cell lines, and importantly, in case of human lymphocytes, the cell growth inhibition percentage decreases drastically (more than 80%), either in the presence of **F3** (containing only MTX) or **F4** (containing FA and MTX). **F4** even promotes human lymphocytes growth, presumably due to the presence of FA, which acts as a metabolite. Thus, the nanodevices exhibited a favorable discrimination between healthy and diseased cells.

Acknowledgments

This research was carried out with the support of Grants 81924 from CONACyT, IN101109 from PAPIIT and 4316 from ICyTDF. The authors kindly thank Gerardo Cedillo Valverde and Carmen Márquez for their technical assistance.

Appendix A. Supplementary material

Supplementary data associated with this article can be found, in the online version, at doi:10.1016/j.bioorg.2012.01.002.

References

- [1] I.U. Uchegbu, A.G. Schatzlein, *Polymers in Drug Delivery*, first ed., Taylor and Francis Group, Florida, 2006.
- [2] Y. Matsumura, H. Maeda, *Cancer Res.* 46 (1986) 6387–6392.
- [3] H. Maeda, L.W. Seymour, Y. Myamoto, *Bioconjugate Chem.* 3 (1992) 351–362.
- [4] D.F. Baban, L.W. Seymour, *Adv. Drug Delivery Rev.* 34 (1998) 109–119.
- [5] A. D'Emanuele, D. Attwood, *Adv. Drug Delivery Rev.* 57 (2005) 2147–2162.
- [6] R. Jevprasesphant, J. Penny, D. Attwood, A. D'Emanuele, *J. Control. Rel.* 97 (2004) 259–267.
- [7] J. Hu, Y. Cheng, Y. Ma, Q. Wu, T. Xu, *J. Phys. Chem. B* 113 (2009) 64–74.
- [8] L. Brannon-Peppas, J.O. Blanchette, *Adv. Drug Delivery Rev.* 56 (2004) 1649–1659.
- [9] J.R. Baker Jr., *Hematology* 1 (2009) 708–719.
- [10] E.R. Gillies, J.M.J. Fréchet, *Drug Discov. Today* 10 (2005) 35–43.
- [11] A.W. Bosman, H.M. Janssen, E.W. Meijer, *Chem. Rev.* 99 (1999) 1665–1688.
- [12] T. Ooya, J. Lee, K. Park, *Bioconjugate Chem.* 15 (2004) 1221–1229.
- [13] Y. Zhang, T.P. Thomas, K. Lee, M. Li, H. Zong, A.M. Desai, A. Kotlyar, B. Huang, M.M.B. Holl, J.R. Baker Jr., *Bioorg. Med. Chem.* 19 (2011) 2557–2564.
- [14] C. Kojima, K. Kono, K. Maruyama, T. Takagishi, *Bioconjugate Chem.* 11 (2000) 910–917.
- [15] A.K. Patri, I.J. Majoros, J.R. Baker Jr., *Curr. Opin. Chem. Biol.* 6 (2002) 466–471.
- [16] I.J. Majoros, A. Myc, T. Thomas, C.B. Mehta, J.R. Baker Jr., *Biomacromolecules* 7 (2006) 572–579.
- [17] J.F. Kukowska-Latallo, K.A. Candido, Z. Cao, S.S. Nigavekar, I.J. Majoros, T.P. Thomas, L.P. Balogh, M.K. Khan, J.R. Baker Jr., *Cancer Res.* 65 (2005) 5317–5324.
- [18] I.J. Majoros, T.P. Thomas, C.B. Mehta, J.R. Baker Jr., *J. Med. Chem.* 48 (2005) 5892–5899.
- [19] A. Monks, D. Scudiero, P. Skehan, R. Shoemaker, K. Paul, D. Vistica, C. Hose, J. Langley, P. Cronise, A. Vaigro-Wolff, M. Gray-Goodrich, H. Campbell, J. Mayo, M. Boyd, *J. Natl. Cancer I* 38 (1991) 757–766.
- [20] A.E. Beezer, A.S.H. King, I.K. Martin, J.C. Mitchell, L.J. Twyman, C.F. Wain, *Tetrahedron* 59 (2003) 3873–3880.
- [21] G.R. Newkome, G.R. Baker, S. Arai, J.M. Saunders, P.S. Russo, K.J. Theriot, C.N. Moorefield, L.E. Rogers, J.E. Miller, T.R. Lieux, M.E. Murray, B. Phillips, L.J. Pascal, *J. Am. Chem. Soc.* 12 (1990) 8458–8465.
- [22] G.R. Newkome, C.N. Moorefield, F. Vögtle, *Dendritic Molecules; Concepts, Syntheses, Perspectives*, first ed., VCH, Weinheim, Germany, 1996.
- [23] C. Griffin, N. Sharda, D. Sood, J. Nair, J. McNulty, S. Pandey, *Cancer Cell Int.* 10 (2007) 1–7.
- [24] R.K. Kainthan, D.E. Brooks, *Biomaterials* 28 (2007) 4779–4787.